Soft Matter

Cite this: *Soft Matter*, 2012, **8**, 6646

www.rsc.org/softmatter

PAPER

Lipid-core nanocapsules: mechanism of self-assembly, control of size and loading capacity

Denise S. Jornada,[a] Luana A. Fiel,[a] Kelly Bueno,[a] Josepe F. Gerent,[a] Cesar L. Petzhold,[b] Ruy C. R. Beck,[ac] Sílvia S. Guterres[ac] and Adriana R. Pohlmann*[abc]

Received 31st March 2012, Accepted 25th April 2012
DOI: 10.1039/c2sm25754h

Nanotechnology in pharmaceutics has the potential to improve drug efficacy by influencing drug distribution in tissues. Nanocarriers have been developed as drug delivery systems to be administered by different biological routes. To ensure the nanotechnological properties, pre-formulation studies are especially critical in determining the influence of the process parameters on the size and polydispersity of particles. Thus, the objective of this work was to establish the mechanism of self-assembly, by determining the influence of the critical aggregation concentration of the materials in the organic phase on the final average particle size and polydispersity of polymeric lipid-core nanocapsules obtained by interfacial deposition of polymer. Measurements of the surface tension and viscosity of the organic and aqueous phases were correlated with the particle size and the concentration of raw materials. We demonstrated that the lipid-core nanocapsules are formed on the nanoscopic scale as unimodal distributions, if the aggregation state of raw materials in the organic phase tends to infinite dilution. The strategy for controlling the particle size distribution is a valuable tool in producing lipid-core nanocapsule formulations with different loading capacities intended for therapeutics.

Introduction

In the past 30 years, pharmaceutical nanotechnology has been devoted to producing new nanocarriers to improve the therapeutic benefits of drugs. In general, nanoencapsulation provides control of drug release rates in specific sites of action, improves drug efficacy, reduces toxicity and delays chemical or enzymatic degradation of the drug.[1–3] Different polymeric nanoparticles have been developed as drug delivery systems to be administered by intravenous, ocular, oral and cutaneous routes.[1,2,4,5]

Polymeric nanospheres and nanocapsules are prepared either by *in situ* polymerization, which includes polymerization in emulsion and interfacial polymerization,[1] or by polymer self-assembly, such as nanoprecipitation and interfacial deposition of the polymer,[3] salting-out[6] and emulsification–diffusion.[7] In all cases, an organic and an aqueous phase are used to structure the supramolecular colloidal suspensions.

To ensure the nanotechnological characteristics of polymeric nanoparticles, several pre-formulation studies were conducted to determine the influence of the process parameters on the size and polydispersity of particles.[8–12] In this way, the homogeneity of the population on the nanometric scale, the average size and the polydispersity are key characteristics to reach potential applicable formulations in therapeutics. So, the ability to cross biological barriers in a selective manner is dependent on the control of the granulometry and the homogeneity of particle sizes.

Considering the emulsification–diffusion method, control of the final particle size is dependent on the initial size of the primary emulsion.[13] Regarding the industrial scale-up of the nanoprecipitation process, the best nanoparticle yields were reached when the polymer concentration was in a semi-dilute regime in the organic phase.[14] In addition, the nanoparticle diameter and polydispersity decreased when lower molar masses and lower polymer concentrations were used, as a consequence of the viscosity of the organic solutions. On the other hand, when preparing nanospheres by the solvent displacement method, the nucleation rate, after mixing the phases, was correlated to the super-saturation rate of the polymer in the organic phase.[11]

Lipid-core nanocapsules (LNCs) have been prepared by interfacial deposition of poly(ε-caprolactone) using a dispersion of lipophilic materials as the core.[15,16] LNCs encapsulating different drugs showed promising biological effects in acute and chronic inflammation,[17,18] multiform glioblastoma[18,19] and neuroinflammation.[20] Resveratrol was accumulated in the brain, liver and spleen after IP (intraperitoneal) or oral administration of drug-loaded LNCs.[21]

The capability of nanoparticles to extravasate biological barriers is related to their size distribution, average size, shape

[a]*Programa de Pós-Graduação em Ciências Farmacêuticas, Faculdade de Farmácia, Universidade Federal do Rio Grande do Sul (UFRGS), Porto Alegre, RS, Brasil. Fax: (+55 51) 3308 5243; Tel: (+55 51) 3308 5215*
[b]*Departamento de Química Orgânica, Instituto de Química, Universidade Federal do Rio Grande do Sul (UFRGS), BPox 15003, 91501-970 Porto Alegre, RS, Brasil. Fax: (+55 51) 3308 7304; Tel: (+55 51) 3308 7237*
[c]*Centro de Nanociência e Nanotecnologia (CNANO-UFRGS), Porto Alegre, RS, Brasil. Tel: (+55 51) 3308 6489*

and surface chemistry. So, our previous results motivated us to investigate the basis for the control of the granulometry and the homogeneity of particle sizes in LNC formulations. Up to now, there has been a lack of information concerning the mechanism of self-assembly to produce lipid-core nanocapsule aqueous formulations. Thus, our objective was to investigate the influence of the critical aggregation concentration of the materials in the organic phase on the control of the average size and polydispersity of lipid-core nanocapsules obtained by interfacial deposition of polymer. Our hypothesis also considered that different particle number densities could be obtained after knowing the physico-chemical basis of this process, and as a consequence, it could be possible to increase the drug loading capacity of the liquid formulation by increasing its particle number density, maintaining the narrow size distribution on the nanoscale. Briefly, we aimed to establish the basis of the preparation of LNCs to control their granulometry, even varying the particle number density of the formulations with a view to developing innovative nanomedicines.

Experimental

Materials

Poly(ε-caprolactone) (PCL) (Mw = 65 000) and Span 60® (sorbitan monostearate) were obtained from Sigma. Capric/caprylic triglyceride (CCT) and polysorbate 80 [poly-(ethyleneglycol)sorbitan monooleate] were purchased from Delaware (Porto Alegre, Brazil). Indomethacin was purchased from DEG (Brazil). All other chemicals and solvents were of analytical or pharmaceutical grade. All reagents were used as received.

Methods

Preparation of lipid-core nanocapsule formulations. Different amounts of materials were used to produce two series of 7 formulations each. The proportions of sorbitan monostearate, oil and polymer were fixed at 1.0 : 4.1 : 2.6 (w/w/w) as previously determined optimal proportions.[16] Series **A** was prepared by varying the amount of polymer (10 to 350 mg), sorbitan monostearate (3.8 to 134.6 mg) and oil (16 to 552 μL), maintaining constant the amount of polysorbate 80 at 77 mg, while series **B** was obtained by varying the amount of all the materials and polysorbate 80 between 7.7 and 269.5 mg.

The experimental procedure consisted of preparing organic phases composed of polymer, oil (capric/caprylic triglyceride) and sorbitan monostearate dissolved in acetone (25 mL) at 37 °C. In separate flasks, polysorbate 80 was dispersed in water (50 mL) at room temperature (aqueous phases). Each organic phase was injected into an aqueous phase under magnetic stirring at room temperature, instantaneously forming a turbid solution. After 10 min, acetone was eliminated and each colloidal suspension concentrated under reduced pressure (40 °C). The final volume of each formulation was adjusted to 10 mL.

The concentrations of polysorbate 80 in water and the polymer in acetone were the basis for naming of the samples, for example: the formulation $\mathbf{A}_{0.4}$ was prepared with 10 mg polymer in 25 mL acetone, using 3.8 mg sorbitan monostearate and 16 μL oil (Table 1). So, the index 0.4 represents concentration of the polymer in the organic phase.

To validate the model, series **C** (3 formulations) was also prepared. These formulations were obtained as described above, using concentrations of materials comprised in a dilute regimen during nanoprecipitation. To determine the influence of the viscosity of the organic phase on the average size, C_{4d} was prepared using 0.100 g polymer, 0.0385 g sorbitan monostearate, 0.158 mL oil, 0.077 g polysorbate 80, 250 mL acetone and 500 mL water. The final volume was adjusted to 10 mL of suspension. Furthermore, C_{10d} and C_{14d} formulations were prepared considering the critical aggregation concentration of the materials in the organic phase (Table 2).

To validate our hypothesis that it could be possible to increase the loading capacity of the liquid formulation by increasing the particle number density, series **D** (3 formulations) was also prepared using indomethacin as a model drug, and $\mathbf{B}_{12}$ was prepared as a control (Table 3). This series was prepared as described above, adding indomethacin in the organic phase. Formulations were prepared in triplicate batches.

Physicochemical characterization of lipid-core nanocapsules

Size analysis by light scattering. Measurements of *z*-average size (mean hydrodynamic diameter) and polydispersity index (relative variance) were performed at 25 °C by dynamic light scattering using backscatter detection at 173° (Zetasizer ZS, Malvern, UK). Each formulation (20 μL) was diluted in 10 mL of ultrapure water (Millipore®, 0.45 μm).

In order to establish a correlation between the final *z*-average size and the mean size obtained just after injecting the organic phase into the aqueous phase (before solvent evaporation), each turbid solution was directly analyzed (without dilution or filtration) (Zetasizer ZS, Malvern, UK). So, different refractive indices for the continuous phases were set for each analysis. When the diluted formulations were analyzed, the refractive index of water (1.330) was used to calculate the size distribution profiles, whereas when the turbid solution (before eliminating

Table 1 Name and composition of the formulations (final volumes of 10 mL)

Formulation[a]	PCL (g)	SM (g)	Oil (mL)	Polysorbate 80 (g)
Series **A**				
$A_{0.4}$	0.0100	0.0038	0.0160	0.0770
A_1	0.0250	0.0096	0.0390	0.0770
A_2	0.0500	0.0192	0.0790	0.0770
A_4	0.1000	0.0385	0.1580	0.0770
A_6	0.1500	0.0577	0.2370	0.0770
A_{10}	0.2500	0.0962	0.3940	0.0770
A_{14}	0.3500	0.1346	0.5520	0.0770
Series **B**				
$B_{0.4}$	0.0100	0.0038	0.0160	0.0077
B_1	0.0250	0.0096	0.0390	0.0193
B_2	0.0500	0.0192	0.0790	0.0385
B_4	0.1000	0.0385	0.1580	0.0770
B_6	0.1500	0.0577	0.2370	0.1155
B_{10}	0.2500	0.0962	0.3940	0.1925
B_{14}	0.3500	0.1346	0.5520	0.2695

[a] Poly(ε-caprolactone) (PCL); sorbitan monostearate (SM); caprylic/capric triglyceride (oil).

Table 2 Composition of the $\mathbf{C}_{10d}$ and $\mathbf{C}_{14d}$ (final volume of 10 mL)

Formulation[a]	PCL (g)	SM (g)	Oil (mL)	Polysorbate 80 (g)	Acetone (mL)	Water (mL)
C_{10d}	0.2500	0.0962	0.3940	0.1925	63	125
C_{14d}	0.3500	0.1346	0.5520	0.2695	88	175

[a] Poly(ε-caprolactone) (PCL); sorbitan monostearate (SM); caprylic/capric triglyceride (oil).

acetone) was analyzed, the dispersant medium refractive index used was 1.356, corresponding to the acetone–water mixture.

Granulometric profiles by laser diffractometry. The granulometric profile of each formulation was carried out at 25 °C by laser diffractometry (Mastersizer 2000, Malvern, UK). Each sample was added directly into the dispersion accessory containing about 100 mL distilled water to obtain obscuration levels between 0.02 and 0.10. The background signal was measured before each analysis.

Surface tension of the organic phase. The surface tension of the different organic phases used to prepare the series of formulations was determined at 20 °C ± 1 by the Wilhelmy plate method using a Tensiometer DCAT 11 (Dataphysics, Germany).

Viscosity analysis of the organic and aqueous phases. The kinetic viscosity of the organic phases (series **A** and **B**) was determined using a vibrational viscometer (SV-10, A&D Company, Japan). Briefly, after the complete dissolution of all materials in the organic phase, the kinetic viscosity was measured (n = 6) at a temperature of 37 ± 0.5 °C. All solutions were prepared in triplicate batches. So, the results are expressed as mean values and standard deviations of 18 measurements for each sample.

The kinetic viscosity of the aqueous phases used to prepare the formulations (series **B**) was determined using the same methodology as described above, but at a temperature of 25 ± 1 °C. The solutions of polysorbate 80 were prepared by dispersing the surfactant (0.0077 g to 0.2695 g) in 50 mL of ultrapure water. So, the range of concentrations studied varied from 0.150 mg mL^{-1} to 5.39 mg mL^{-1}.

To determine the viscosity for dynamic light scattering (DLS) analysis, diluted samples at 0.0003 mg mL^{-1} and 0.0108 mg mL^{-1} were also used.

Nanoparticle tracking analysis (NTA). Analyses by NTA were carried out using the NanoSight (NanoSight, Amesbury, England), equipped with a sample chamber containing a 640 nm laser and a fluoroelastomer Viton O-ring. The samples were injected into the sample chamber with a syringe. All measurements were performed at room temperature. The software used to capture and analyze data was the NTA 2.0 Build 127. The samples were evaluated for 60 s with the manual shutter and gain settings.

This technique combines light scattering microscopy with a laser camera charge-coupled device (CCD), which allows viewing and recording nanoparticles in solution. The NTA software is able to identify and track individual nanoparticles, which are in Brownian motion, and relate this movement to particle size, according to the following equation derived from the Stokes–Einstein equation (eqn (1)).

$$\overline{(x,y)^2} = \frac{2K_bT}{3r_h\pi\eta} \quad (1)$$

Drug quantification. The colloidal suspensions were treated with acetonitrile, resulting in the dissolution of the formulation components. The assay of indomethacin was performed by high performance liquid chromatography (HPLC) according to the methodology previously validated for linearity, precision, reproducibility, accuracy, limit of quantification, selectivity and specificity.[17]

Analyses were performed on a Perkin Elmer Series 200 chromatograph, using an ultraviolet visible detector (λ = 267 nm), a guard-column and a Nova-Pak C-18 column (150 mm, 4.9 mm, 4 μm – Waters), a flow of 0.8 mL min^{-1} and an isocratic mobile phase of acetonitrile : water (70 : 30, v/v) adjusted to an apparent pH of 5.0 ± 0.5 with 10% (v/v) acetic acid.

Results

Series **A** and series **B** formulations were obtained as white milky liquids, whose sizes (*z*-average) ranged from 149 to 398 nm (**A**) and from 128 to 351 nm (**B**). So, in all cases nanoscopic populations were obtained by varying the concentrations of sorbitan monostearate, oil and polymer at constant proportions of 1 : 4.1 : 2.6 (w/w/w) in the formulations.

Table 3 Composition of the $\mathbf{D}_{4a}$, $\mathbf{D}_{4b}$, $\mathbf{B}_{12}$ and $\mathbf{D}_{12b}$ (final volume of 10 mL)

Formulation[a]	PCL (g)	SM (g)	Oil (mL)	Polysorbate 80 (g)	Drug (g)	Acetone (mL)	Water (mL)
D_{4a}	0.1000	0.0385	0.1580	0.0770	0.0050	25	50
D_{4b}	0.1000	0.0385	0.1580	0.0770	0.0150	25	50
B_{12}	0.3000	0.1155	0.4740	0.2310	0	75	150
D_{12b}	0.3000	0.1155	0.4740	0.2310	0.0150	75	150

[a] Poly(ε-caprolactone) (PCL); sorbitan monostearate (SM); caprylic/capric triglyceride (oil).

Considering that bottom-up strategies are based on self-assembly driven by the Marangony effect, surface tension is an important parameter for controlling the mean size of the particles, particularly when the emulsification–diffusion method is used.[12,22] Furthermore, previous reports stated that the final mean size of the nanoparticles obtained by the nanoprecipitation technique depends on the viscosity of the organic phase.[6,8,23] Based on those reports, in the present work the surface tension and the kinetic viscosity of the organic and aqueous phases used to prepare the formulations (series **A** and series **B**) were determined.

The surface tension of the organic phase was nearly constant between 23.232 and 23.417 mN m^{-1} after varying the concentrations of polymer, oil and sorbitan monostearate, while the aqueous phases, containing different concentrations of polysorbate 80 (series **B**), showed surface tension values ranging from 42.087 to 39.461 mN m^{-1} (Fig. 1). The higher the concentration of this surfactant, the lower the surface tension was. Considering that ultrapure water has a surface tension value of 71.580 mN m^{-1}, micelles are present in all aqueous phases before injecting each organic phase. The results showed that no correlation between the final nanoscopic size of the formulations and the surface tension of the organic or aqueous phases was observed. These results suggested that water is not present in the core dispersion even though the LNCs are composed from a dispersion of lipids as the core, surrounded by a polymer wall. Previous results showed the absence of water in the core of those nanocapsules by fluorimetry, comparing dye-labeled to dye-loaded nanocapsules.[24] On the contrary, when a primary emulsion is formed to generate the nanoparticles using the emulsification–diffusion method, the final particle size is linearly correlated with the organic phase surface tension coefficient.[12,13]

Following our study, the kinetic viscosities of the organic and aqueous phases were determined. Regarding the aqueous phases, all solutions presented viscosity values between 0.88 and 0.90 mPa s independently of the concentration of polysorbate 80. Considering that ultrapure water had a viscosity of 0.89 under the same experimental conditions, and that the standard deviations of all measurements ranged between 0.01 and 0.02, the final particle sizes were not dependent on the viscosity of the aqueous phases. On the other hand, the organic phases presented increasing viscosities with the increase in concentration of the raw materials (Table 4). In addition, the final particle sizes were directly proportional to the viscosity (Fig. 2).

Regarding both series (**A** and **B**), the lowest concentrations of the raw materials showed similar particle sizes, while the highest values showed discrepancies in mean size between the series (Fig. 2). In the same way, the relative variance [polydispersity index (PDI)] obtained by DLS was lower than 0.20 for the lowest concentrations, while the PDI ranged from 0.26 to 0.44 for the higher concentrations of components.

To verify if the mean size of the LNC can be modulated by decreasing the concentrations of the raw materials and increasing the solvent volume, a new formulation ($\mathbf{C}_{4d}$) was prepared using the same amounts of materials used for $\mathbf{B}_4$ (or $\mathbf{A}_4$) but higher amounts of acetone (250 mL) and water (500 mL). In this case, the concentrations of the raw materials before the evaporation step corresponded to the $\mathbf{B}_{0.4}$ formulation. As a result, $\mathbf{C}_{4d}$

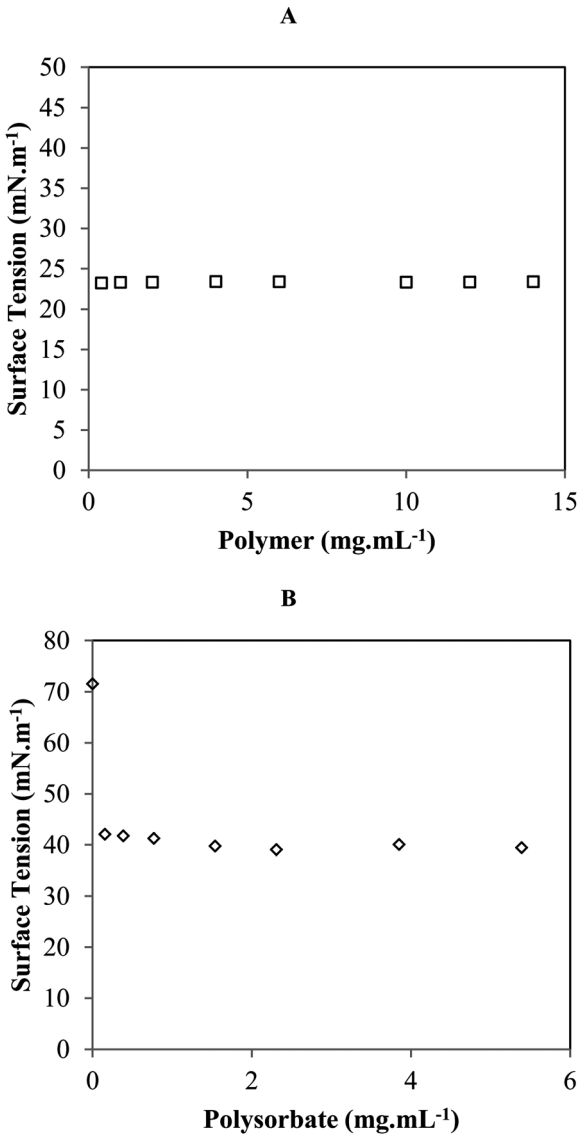

Fig. 1 (A) Mean values and standard deviation of the surface tension of the organic phase as a function of the concentrations of polymer, oil and sorbitan monostearate (plotted against polymer concentration), and (B) mean values and standard deviation of the surface tension of the aqueous phase as a function of the concentration of polysorbate 80.

Table 4 Kinetic viscosities of the organic phases used to prepare series **A** and **B**. Concentrations are expressed as amounts of material per volume of acetone solution[a]

PCL (mg mL^{-1})	SM (mg mL^{-1})	Oil (μL mL^{-1})	Viscosity (mPa s)
0.4	0.154	0.63	0.32 ± 0.00
1.0	0.385	1.58	0.32 ± 0.03
2.0	0.769	3.15	0.36 ± 0.03
4.0	1.538	6.31	0.36 ± 0.03
6.0	2.308	9.46	0.41 ± 0.03
10.0	3.846	15.77	0.46 ± 0.03
14.0	5.385	22.08	0.57 ± 0.02

[a] Poly(epsilon-caprolactone) (PCL); sorbitan monostearate (SM); caprylic/capric triglyceride (oil).

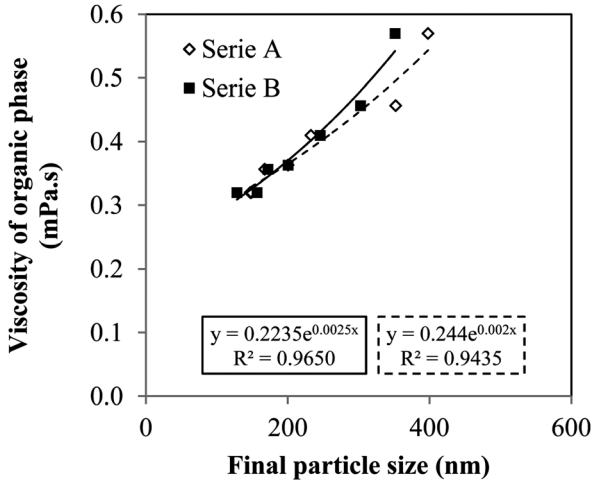

Fig. 2 Correlation between the final particle sizes of series **A** or series **B** and the viscosity of the organic phases.

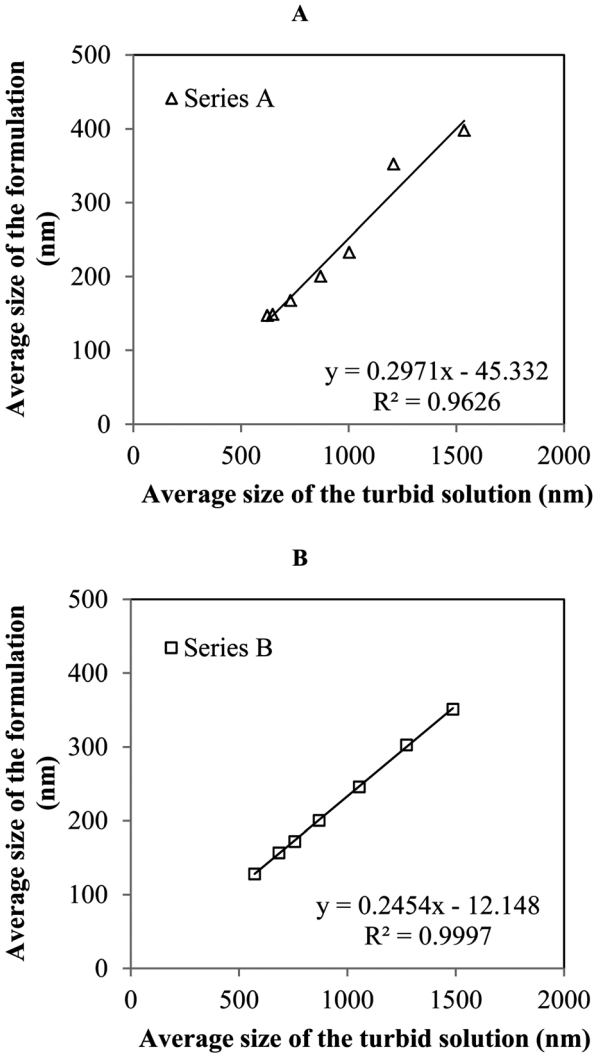

Fig. 3 Correlation between the average particle sizes of formulations and the average size of the turbid solutions (obtained just after injection of the organic phase into the aqueous phase, before solvent evaporation) for series **A** and series **B**.

showed mean particle sizes (129 nm) smaller than the mean size of the $\mathbf{B}_4$ formulation (201 nm). Likewise, the $\mathbf{C}_{4d}$ formulation has a similar average particle size to the $\mathbf{B}_{0.4}$ formulation (128 nm), despite the proportions of the final particle number density being 10 : 1.

Previously, it was demonstrated that the viscosity of the organic phase influenced the final mean size of the nanospheres.[10] That result was attributed to an increase in the nanodrop size formed during the process of nanoprecipitation. Considering these findings, and that the discrepancies in size mentioned above could be related to the agglomeration of nanocapsules, leading to an increase in the mean size and polydispersity index, the final average particle sizes by DLS were compared to the size of the nanocapsules just after injecting the organic phase into the aqueous phase before eliminating the organic solvent (turbid solution) (Fig. 3).

Linear correlations were obtained for both series (**A** and **B**) when the final particle size was plotted against the size of the turbid solution, indicating that the nanocapsules were formed just after adding the organic phase to the aqueous phase and that the nanocapsules reduced their size after acetone evaporation. The larger size of the particles before eliminating acetone might be a consequence of organic solvent diffusion through the polymeric wall, which was previously observed for ethanol.[25,26]

The use of different concentrations of polysorbate 80 affected the linearity by producing a better correlation for series **B**, in which this concentration varied proportionally to the materials solubilized in the organic phase. The results indicated that the final particle sizes of the LNCs depended on the initial concentrations of materials in the organic and aqueous solutions. The granulometric profiles of series **A** and **B** ranging from 40 nm to 2 mm were determined by laser diffraction (Table 5). For series **A**, whose formulations were prepared with a constant concentration of polysorbate 80, D[4,3] was independent of the concentration of this surfactant, while for series **B**, whose polysorbate 80 concentration was varied to maintain a constant proportionality in relation to the other raw materials, D[4,3] increased with the increase in concentration of this surfactant. The high concentration of polysorbate 80 coating in $\mathbf{A}_{0.4}$ could promote the formation of micelles of surfactant, whose agglomerate led to an increase in D[4,3]. The best formulation was $\mathbf{A}_4$ ($\mathbf{B}_4$) having D[4,3] of 243 nm and span of 1.63. Considering these data, series **B** was prepared, taking into account the proportionality of $\mathbf{A}_4$ (1.0 : 4.1 : 2.6 : 2.0 of PCL, SM, CCT and polysorbate 80, respectively). Then, the results showed clearly that D[4,3] and polydispersity increased with the increase in volume fraction of the LNCs, corroborating the results described above. Formulations prepared with a lower particle number density ($\mathbf{B}_{0.4}$ to $\mathbf{B}_6$) presented D[4,3] lower than 358 nm (Table 4), while formulations prepared with the highest volume fractions ($\mathbf{B}_{10}$ and $\mathbf{B}_{14}$) showed D[4,3] values of 1.14 and 2.10 μm, respectively. Regarding the polydispersity, $\mathbf{B}_{0.4}$ to $\mathbf{B}_6$ formulations had span lower than 1.63, whereas $\mathbf{B}_{10}$ and $\mathbf{B}_{14}$ were polydispersed systems with a span of 4.1 and 9.1 (Table 5).

Up to this point, the concentrations of raw materials in the organic phase seemed the most important factor in controlling

Table 5 Particle size distributions of series **A** and **B** formulations determined by laser diffractometry

Formulations	D[4,3] μm	d(0,1) μm	d(0,5) μm	d(0,9) μm	Span
Series **A**					
$A_{0.4}$	23.300	0.092	0.191	60.800	318.300
A_1	7.061	0.087	0.159	0.377	1.821
A_2	0.630	0.072	0.142	0.270	1.389
A_4	0.243	0.093	0.213	0.441	1.633
A_6	0.398	0.170	0.340	0.690	1.531
A_{10}	0.754	0.217	0.457	1.234	2.227
A_{14}	0.232	0.074	0.170	0.458	2.258
Series **B**					
$B_{0.4}$	0.134	0.080	0.127	0.200	0.948
B_1	0.169	0.074	0.140	0.255	1.294
B_2	0.165	0.069	0.143	0.289	1.540
B_4	0.243	0.093	0.213	0.441	1.633
B_6	0.358	0.150	0.323	0.622	1.458
B_{10}	1.139	0.247	0.581	2.600	4.075
B_{14}	2.100	0.096	0.542	5.000	9.094

the size distribution and polydispersity of the LNCs. Considering the concentration of the materials before and after eliminating acetone, as well as comparing the results of series **A** and **B** with the C_{4d} formulation, the concentration of the materials in the organic phase is the most influencing parameter in obtaining a narrow nanoscopic final particle size. So, the production of LNCs, with control of the mean size and a narrow size distribution, might be related to the aggregation state of the raw materials in the organic phase (acetone). Despite the differences in the supramolecular structure of the colloids, this hypothesis is based on previous reports showing the influence of the aggregation state of the organic phase on the final distribution size of the nanospheres.[14] So, narrow size distributions of LNCs with mean particle sizes on the nanoscopic scale could be reached by selecting the concentrations of the raw materials in the organic phase, maintaining their optimized proportionality.

When the polymer is in a dilute regimen, the chains are independent; hence the aqueous phase diffuses into the organic phase, triggering the formation of isolated clusters, which have smaller and defined sizes. The opposite situation occurs in semi-dilute solutions, due to the overlapping of polymer chains forming larger and more varied clusters.[26] Both examples were only demonstrated for nanospheres, whose supramolecular structures correspond to polymeric matricial systems, produced from an acetone solution of polymer (PCL) injected into distilled water.[14]

Nevertheless, the critical aggregation concentration is an important factor in controlling the size and polydispersity of LNC formulations. The main constituent which contributes to the viscosity in the organic phase is PCL. So, to determine the critical aggregation concentration, the solution was prepared with all the materials (polymer, oil and surfactant) and the viscosity of the organic phase was plotted as a function of the logarithm of the concentration of the polymer in the organic phase (Fig. 4). The differences in molecular aggregation state were demonstrated by the dependence of the viscosity of the organic phase by varying the concentration of the components in solution. In addition, since the boundary between the dilute and semi-dilute solutions can be determined by calculating the intrinsic viscosity of a polymer solution,[14] linear equations were fitted to establish the correlation between the logarithm of the concentration of polymer and the viscosity. In this case, the linear correlations ($r = 0.9066$ and $r = 0.9544$) at dilute and semi-dilute regimens were found, respectively (eqn (2) and (3)).

$$\eta = 0.0493 \log[\text{PCL}] + 0.3338 \quad (2)$$

$$\eta = 0.3523 \log[\text{PCL}] + 0.1394 \quad (3)$$

After equaling the equations, the critical aggregation concentration of PCL was determined as 4.38 mg mL^{-1} in acetone. Hence, to maintain the proportionality of the materials, the concentrations of oil and sorbitan monostearate in that organic phase corresponded to 6.92 mg mL^{-1} and 1.69 mg mL^{-1}, respectively. Control of the size and polydispersity was achieved when a dilute regimen was used in the organic phase. So, the results clearly demonstrated, for the first time, that nanocapsules are formed on the nanoscopic scale as unimodal distributions, if

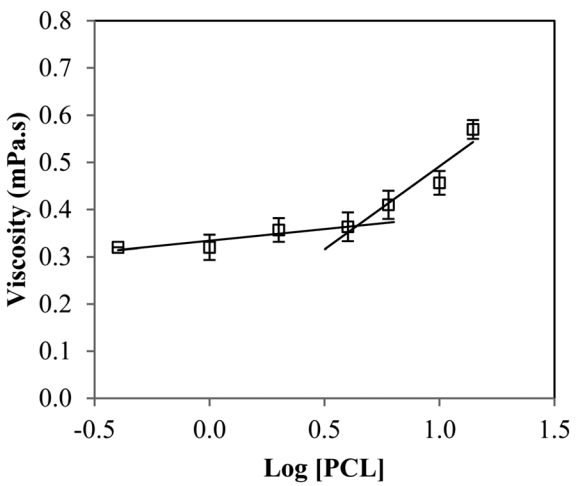

Fig. 4 Viscosity of the organic phase (η) as a function of the logarithm of the polymer concentration.

the aggregation state of the raw materials in the organic phase tends to infinite dilution.

If a dilute regimen controlled the granulometric profile of the LNCs, it could be possible to prepare formulations with higher volume fractions, by controlling the concentration of the materials in the organic and aqueous solutions. So, to evaluate the feasibility of nanotechnological formulations, with the highest volume fractions presenting homogeneous, unimodal and nanoscopic populations of LNCs, $\mathbf{C}_{10d}$ and $\mathbf{C}_{14d}$ were prepared using a dilute regimen in the organic phase, by increasing the amount of solvent during preparation (Table 2). For both formulations, the concentrations of materials in acetone were 4.0 mg mL^{-1} (PCL), 1.5 mg mL^{-1} (SM) and 6.2 mg mL^{-1} (oil). All materials were used below the critical aggregation concentration in the organic phase. Moreover, the final concentrations of materials in the $\mathbf{C}_{10d}$ and $\mathbf{C}_{14d}$ aqueous suspensions (after evaporation) were similar to their concentrations in $\mathbf{B}_{10}$ and $\mathbf{B}_{14}$. However, $\mathbf{C}_{10d}$ and $\mathbf{C}_{14d}$ had similar concentrations of materials in the organic phase to the $\mathbf{B}_4$ (or $\mathbf{A}_4$) formulation. Nanoscopic unimodal particle size distributions were determined for the $\mathbf{C}_{10d}$ and $\mathbf{C}_{14d}$ formulations (Fig. 5). The results corroborate the data above indicating that the critical aggregation concentration in the organic phase is the limit to maintain the control of the size and distribution of LNC.

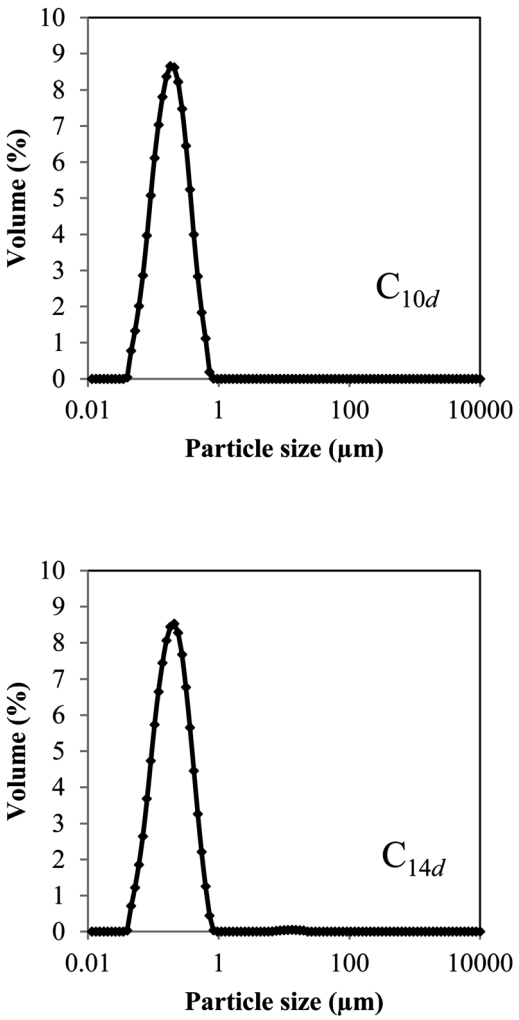

Fig. 5 Granulometric profiles of $\mathbf{C}_{10d}$ and $\mathbf{C}_{14d}$ by laser diffractometry.

To validate the model, we hypothesized that the drug loading capacity could be increased by increasing the particle number density of a given formulation. Indomethacin was chosen as the drug model, because its saturation concentration in LNCs has been previously reported.[28] Therefore, formulation $\mathbf{D}_{4a}$ was prepared with an amount of indomethacin susceptible to complete encapsulation, while formulation $\mathbf{D}_{4b}$ was prepared with an amount of drug that was three times higher. For $\mathbf{D}_{4b}$, drug crystals are expected to be simultaneously formed with the drug-loaded LNC since, in this case, the dispersed pseudo-phase is oversaturated. To validate the hypothesis, formulation $\mathbf{D}_{12b}$ was prepared using the same amount of drug used for $\mathbf{D}_{4b}$ but the dispersed phase has a particle number density three times higher. To obtain these formulations, all materials were used below the critical aggregation concentration in the organic phases.

All formulations presented nanoscopic populations (DLS) with average particle sizes below 250 nm and a low PDI (Table 6). The hydrodynamic diameters observed for the drug-loaded formulations were slightly higher than to those observed for $\mathbf{B}_4$ and $\mathbf{B}_{12}$.

$\mathbf{D}_{4a}$ and $\mathbf{D}_{12b}$ showed a monomodal nanoscopic population by laser diffraction, while $\mathbf{D}_{4b}$ showed the same nanoscopic population and at least two micrometric populations (Fig. 6). As expected, the excess of drug in the formulation generated the microscopic populations observed in the granulometric profile. Crystals of the drug could be formed when saturation was exceeded. Their size is dependent on the supersaturation state and the physico-chemical characteristics of the drug and the raw materials. Nanocrystals can be formed during nanoprecipitation, agglomerating as a function of time.

The scattering intensity of formulations varies when drug nanocrystals are formed simultaneously with the colloids.[27,28] Therefore, NTA is able to characterize colloidal formulations by correlating scattering intensity and hydrodynamic diameter. In order to compare the drug-loaded formulations to the drug-unloaded formulations and determine the presence of nanocrystals in $\mathbf{D}_{4b}$, the scattering intensity *versus* the size distribution of $\mathbf{B}_4$, $\mathbf{B}_{12}$, $\mathbf{D}_{4a}$, $\mathbf{D}_{4b}$ and $\mathbf{D}_{12b}$ was investigated. Drug-unloaded formulations show similar 1D and 2D plots by NTA (Fig. 7) indicating the homogeneity of those formulations. $\mathbf{D}_{4a}$ and $\mathbf{D}_{12b}$ showed similar 2D plots (Fig. 8, A1 and C1) when compared to the drug-unloaded formulations (Fig. 7). On the contrary, a dispersion of dots having a higher light scattering is observed in the 2D plots for $\mathbf{D}_{4b}$ (Fig. 8, B1). This result is observed when

Table 6 Drug contents, particle size and PDI (dynamic light scattering) for $\mathbf{D}_{4a}$, $\mathbf{D}_{4b}$, $\mathbf{B}_{12}$ and $\mathbf{D}_{12b}$ (n = 3)

Formulation	Drug final concentration (mg mL^{-1})	Size (nm)	PDI
B_4	0	200	0.07
D_{4a}	0.54 ± 0.02	239	0,18
D_{4b}	1.55 ± 0.04	217	0,18
B_{12}	0	194	0.09
D_{12b}	1.50 ± 0.01	232	0,17

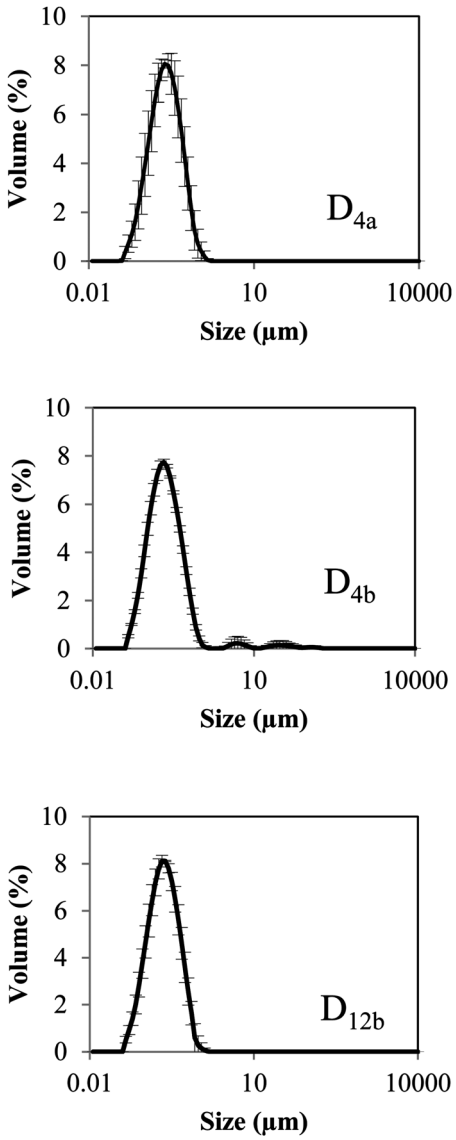

Fig. 6 Granulometric profiles of $\mathbf{D}_{4a}$, $\mathbf{D}_{4b}$ and $\mathbf{D}_{12b}$ by laser diffraction.

drug nanocrystals are simultaneously formed in the formulation. Since the NTA software allows the subtraction of one profile from the other, by selecting the areas of dot dispersion in the 2D plots to generate the 1D plot profile, formulations were compared. Fig. 8 shows dots inside the squares in 2D plots, the selection of which was based on the respective drug-unloaded formulations, $\mathbf{B}_4$ for $\mathbf{D}_{4a}$ and $\mathbf{D}_{4b}$ and $\mathbf{B}_{12}$ for $\mathbf{D}_{12b}$. Some dots representing a higher relative light intensity (dots outside the square) were only observed for $\mathbf{D}_{4b}$, whose 1D plot showed particles ranging from 50 to 250 nm (Fig. 8, B1 and B2). On the other hand, the NTA 2D plots for $\mathbf{D}_{4a}$ or $\mathbf{D}_{12b}$ subtracted from the 2D plots of $\mathbf{B}_4$ or $\mathbf{B}_{12}$, respectively, showed similar profiles (Fig. 8, A1 and A2, C1 and C2). The hypothesis was validated, and a higher drug-loaded capacity was obtained by increasing the particle number density in the formulation. The result observed for $\mathbf{D}_{12b}$ was achieved by using the materials below the critical aggregation concentration in the organic phase, followed by the nanoprecipitation step.

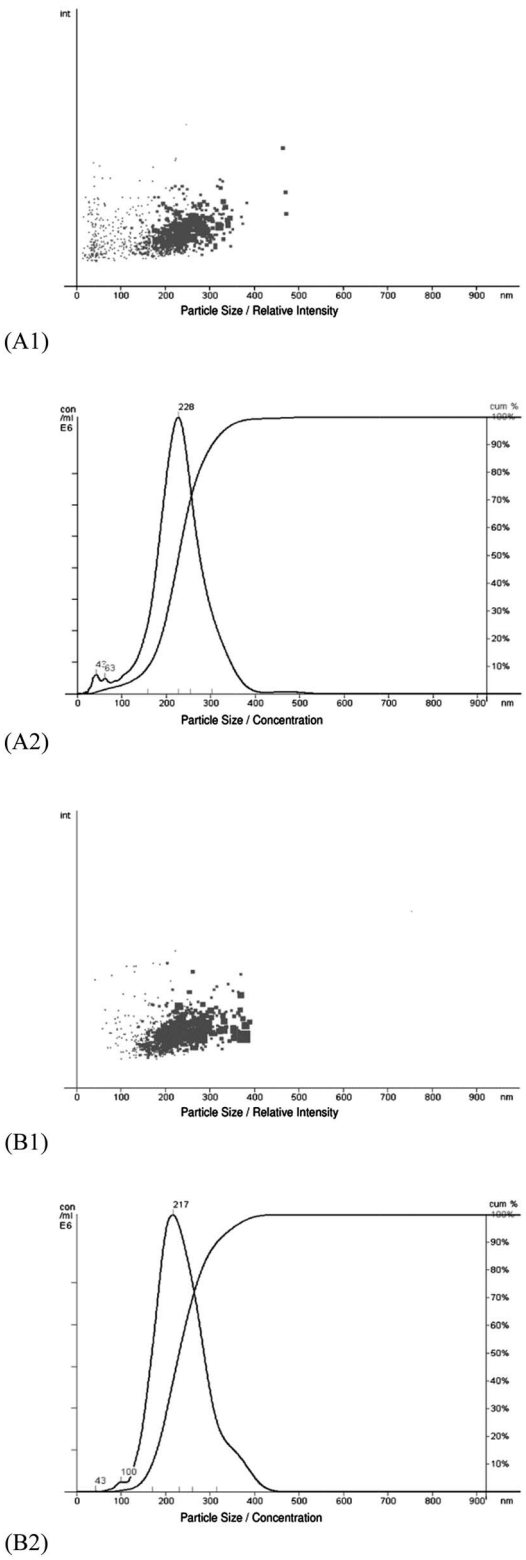

Fig. 7 NTA 2D plots: particle size by relative light intensity for the drug-unloaded formulations of B_4 (A1) and B_{12} (B1) and NTA 1D plots: particle size distribution by concentration of particles for B_4 (A2) and B_{12} (B2).

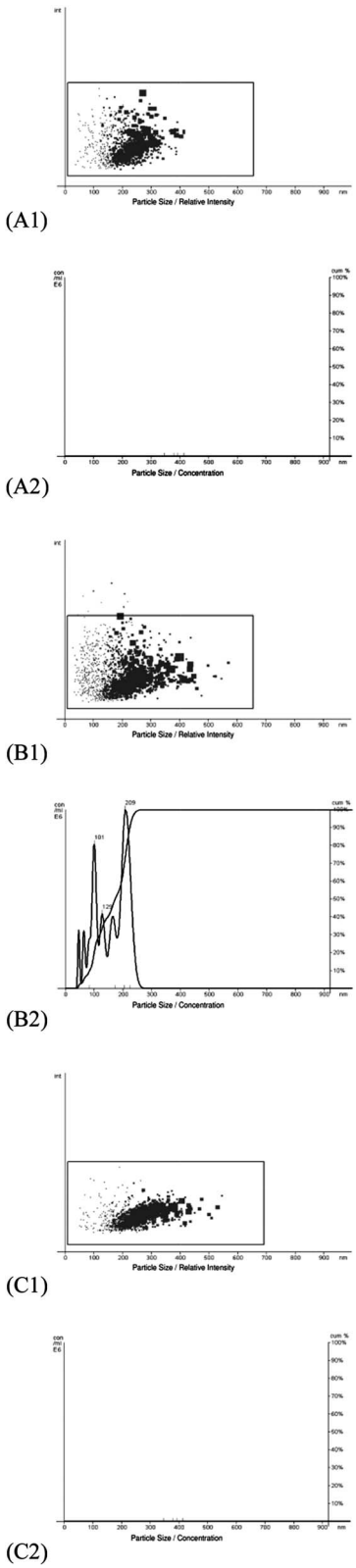

Fig. 8 NTA 2D plots: D_{4a} (A1), D_{4b} (B1) and D_{12b} (C1) presenting dot selection based on the profiles of drug-unloaded formulations. NTA 1D plots: size distribution of dots outside the selection for D_{4a} (A2), D_{4b} (B2) and D_{12b} (C2).

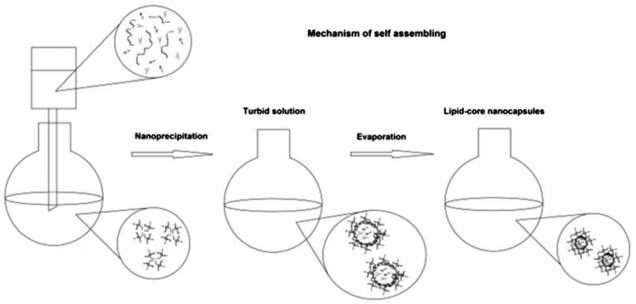

Fig. 9 Illustrative model of the mechanism of the lipid-core nanocapsule formation.

Conclusions

The results demonstrated that there is no correlation between the final size of the lipid-core nanocapsules and the surface tension of the organic or aqueous phases when the colloids are prepared by the interfacial deposition method. Nevertheless, there is a correlation between the concentrations of the raw materials in the organic or aqueous phases and the final particle sizes. The final mean particle size and size distributions are dependent on the range of concentrations of the raw materials in the organic phase, permitting modulation and control of the granulometry of the colloids, using the interfacial deposition of a preformed polymer method. Moreover, the lack or excess of the surfactant used in the aqueous phase is crucial to the stability and the narrow size distribution of the colloid.

For the first time, it has been shown that control of the size and nanotechnological quality of nanocapsules, using the nanoprecipitation method, is dependent on the critical aggregation concentration of the raw materials in the organic phase. Hence, the model of the formation mechanism for obtaining the lipid-core nanocapsules is based on a molecular solution of raw materials, which, in contact with the non-solvent, self-assembles into supramolecular structures, which decrease in size after solvent evaporation (Fig. 9). Considering this model, we were able to increase the particle number density in the formulation, keeping their nanotechnological quality. This result opened up the possibility of increasing the loading capacity of the formulations, which was demonstrated for indomethacin as a drug model. In this way, this report shows that lipid-core nanocapsules are an important platform to encapsulate lipophilic drugs, envisaging drug delivery and drug targeting.

Acknowledgements

Rede Nanobiotecnologia CAPES, CNPq/Brasilia/Brazil, INCT-IF CNPq/MCT, Pronem and Pronex FAPERGS-CNPq, FAPERGS.

References

1 P. Couvreur, G. Barratt, E. Fattal, P. Legrand and C. Vauthier, *Crit. Rev. Ther. Drug Carrier Syst.*, 2002, **19**, 99.
2 C. Vauthier and K. Bouchemal, *Pharm. Res.*, 2009, **26**, 1025.
3 C. E. Mora-Huertas, H. Fessi and A. Elaissari, *Int. J. Pharm.*, 2010, **385**, 113.
4 A. M. Campos, Y. Diebold, E. L. S. Carvalho, A. Sánchez and M. J. Alonso, *Pharm. Res.*, 2004, **21**, 803.

5 S. S. Guterres, M. P. Alves and A. R. Pohlmann, *Drug Target Insights*, 2007, **2**, 147.
6 S. Galindo-Rodriguez, E. Allémann, H. Fessi and E. Doelker, *Pharm. Res.*, 2004, **21**, 1428.
7 D. Quintanar-Guerrero, H. Fessi, E. Allémann and E. Doelker, *Int. J. Pharm.*, 1996, **143**, 133.
8 V. C. F. Mosqueira, P. Legrand, H. Pinto-Alphandary, F. Puisieux and G. Barratt, *J. Pharm. Sci.*, 2000, **89**, 614.
9 C. J. Choi, O. Tolochko and B. K. Kim, *Mater. Lett.*, 2002, **56**, 289.
10 M. Chorny, I. Fishbein, H. D. Danenberg and G. Golomb, *J. Controlled Release*, 2002, **83**, 389.
11 F. Lince, D. L. Marchisio and A. A. Barresi, *J. Colloid Interface Sci.*, 2008, **322**, 505.
12 F. S. Poletto, L. A. Fiel, B. Donida, M. I. Ré, S. S. Guterres and A. R. Pohlmann, *Colloids Surf., A*, 2008, **324**, 105.
13 F. S. Poletto, R. P. Silveira, L. A. Fiel, B. Donida, M. Rizzi, S. S. Guterres and A. R. Pohlmann, *J. Nanosci. Nanotechnol.*, 2009, **9**, 4933.
14 P. Legrand, S. Lesieur, A. Bochot, R. Gref, W. Raatjes, G. Barratt and C. Vauthier, *Int. J. Pharm.*, 2007, **344**, 33.
15 E. Jäger, C. G. Venturini, F. S. Poletto, L. M. Colomé, J. P. U. Pohlmann, A. Bernardi, A. M. O. Battastini, S. S. Guterres and A. R. Pohlmann, *J. Biomed. Nanotechnol.*, 2009, **5**, 130.
16 C. G. Venturini, E. Jäger, C. P. Oliveira, A. Bernardi, A. M. O. Battastini, S. S. Guterres and A. R. Pohlmann, *Colloids Surf., A*, 2011, **375**, 200.
17 L. Cruz, S. R. Schaffazick, T. D. Costa, L. U. Soares, G. Mezzalira, N. P. da Silveira, E. E. S. Schapoval, A. R. Pohlmann and S. S. Guterres, *J. Nanosci. Nanotechnol.*, 2006, **6**, 3154.
18 A. Bernardi, E. Braganhol, E. Jäger, F. Figueiró, M. I. Edelweiss, A. R. Pohlmann, S. S. Guterres and A. M. Battastini, *Cancer Lett.*, 2009, **281**, 53.
19 A. Bernardi, R. L. Frozza, E. Jäger, F. Figueiró, C. Salbego, A. R. Pohlmann, S. S. Guterres and A. M. O. Battastini, *Eur. J. Pharmacol.*, 2008, **586**, 24.
20 A. Bernardi, R. L. Frozza, A. P. Horn, M. M. Campos, J. B. Calixto, C. Salbego, A. R. Pohlmann, S. S. Guterres and A. M. O. Battastini, *Neurochem. Int.*, 2010, **57**, 629.
21 R. L. Frozza, A. Bernardi, K. Paese, J. B. Hoppe, T. Silva, A. M. O. Battastini, A. R. Pohlmann, S. S. Guterres and C. Salbego, *J. Biomed. Nanotechnol.*, 2010, **6**, 694.
22 M. Lappa and C. Piccolo, *Phys. Fluids*, 2004, **16**, 4262.
23 I. L. Blouza, C. Charcosset, S. Sfar and H. Fessi, *Int. J. Pharm.*, 2006, **325**, 124.
24 A. Jäger, V. Stefani, S. S. Guterres and A. R. Pohlmann, *Int. J. Pharm.*, 2007, **338**, 297.
25 C. Mayer, D. Hoffmann and M. Wohlgemuth, *Int. J. Pharm.*, 2002, **242**, 37.
26 A. R. Pohlmann, L. U. Soares, L. Cruz, N. P. da Silveira and S. S. Guterres, *Curr. Drug Delivery*, 2004, **1**, 103.
27 J. Clarke and B. Vincent, *Journal of The Chemical Society, Faraday Transactions 1: Physical Chemistry in Condensed Phases*, 1981, **77**, 1831.
28 A. R. Pohlmann, G. Mezzalira, C. G. Venturini, L. Cruz, A. Bernardi, E. Jäger, A. M. O. Battastini, N. P. Da Silveira and S. S. Guterres, *Int. J. Pharm.*, 2008, **359**, 105.

Addition and correction

Note from RSC Publishing

This article was originally published with incorrect page numbers. This is the corrected, final version.

The Royal Society of Chemistry apologises for these errors and any consequent inconvenience to authors and readers.